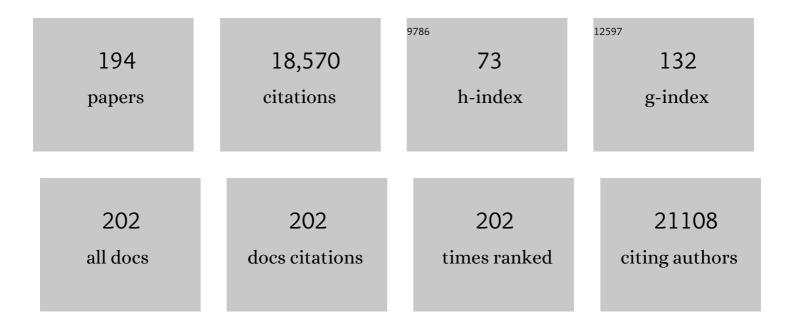
List of Publications by Year in descending order

Source: https://exaly.com/author-pdf/5917815/publications.pdf Version: 2024-02-01



#	Article	IF	CITATIONS
1	Diverse Applications of Nanomedicine. ACS Nano, 2017, 11, 2313-2381.	14.6	976
2	Strongly Photoluminescent CdTe Nanocrystals by Proper Surface Modification. Journal of Physical Chemistry B, 1998, 102, 8360-8363.	2.6	678
3	Superparamagnetic iron oxide nanoparticles: from preparations to in vivo MRI applications. Journal of Materials Chemistry, 2009, 19, 6274.	6.7	610
4	The Influence of Carboxyl Groups on the Photoluminescence of Mercaptocarboxylic Acid-Stabilized CdTe Nanoparticles. Journal of Physical Chemistry B, 2003, 107, 8-13.	2.6	581
5	Synthesis and Characterization of a Size Series of Extremely Small Thiol-Stabilized CdSe Nanocrystals. Journal of Physical Chemistry B, 1999, 103, 3065-3069.	2.6	565
6	Lightâ€Triggered Assembly of Gold Nanoparticles for Photothermal Therapy and Photoacoustic Imaging of Tumors In Vivo. Advanced Materials, 2017, 29, 1604894.	21.0	444
7	Enhancement Effect of Illumination on the Photoluminescence of Water-Soluble CdTe Nanocrystals: Toward Highly Fluorescent CdTe/CdS Coreâ^'Shell Structure. Chemistry of Materials, 2004, 16, 3853-3859.	6.7	386
8	In vivo covalent cross-linking of photon-converted rare-earth nanostructures for tumour localization and theranostics. Nature Communications, 2016, 7, 10432.	12.8	376
9	Aqueous Based Semiconductor Nanocrystals. Chemical Reviews, 2016, 116, 10623-10730.	47.7	364
10	One-Pot Reaction to Synthesize Water-Soluble Magnetite Nanocrystals. Chemistry of Materials, 2004, 16, 1391-1393.	6.7	338
11	Magnetic/Upconversion Fluorescent NaGdF ₄ :Yb,Er Nanoparticle-Based Dual-Modal Molecular Probes for Imaging Tiny Tumors <i>in Vivo</i> . ACS Nano, 2013, 7, 7227-7240.	14.6	336
12	Electroluminescence of different colors from polycation/CdTe nanocrystal self-assembled films. Journal of Applied Physics, 2000, 87, 2297-2302.	2.5	310
13	Enhancing Both Biodegradability and Efficacy of Semiconducting Polymer Nanoparticles for Photoacoustic Imaging and Photothermal Therapy. ACS Nano, 2018, 12, 1801-1810.	14.6	299
14	Ambient Aqueous Synthesis of Ultrasmall PEGylated Cu _{2â^'} <i>_x</i> Se Nanoparticles as a Multifunctional Theranostic Agent for Multimodal Imaging Guided Photothermal Therapy of Cancer. Advanced Materials, 2016, 28, 8927-8936.	21.0	282
15	Receptor-Mediated Delivery of Magnetic Nanoparticles across the Blood–Brain Barrier. ACS Nano, 2012, 6, 3304-3310.	14.6	272
16	BSAâ€Mediated Synthesis of Bismuth Sulfide Nanotheranostic Agents for Tumor Multimodal Imaging and Thermoradiotherapy. Advanced Functional Materials, 2016, 26, 5335-5344.	14.9	255
17	Synthesis and Shape-Tailoring of Copper Sulfide/Indium Sulfide-Based Nanocrystals. Journal of the American Chemical Society, 2008, 130, 13152-13161.	13.7	246
18	Preparation of Water-Soluble Magnetite Nanocrystals from Hydrated Ferric Salts in 2-Pyrrolidone: Mechanism Leading to Fe3O4. Angewandte Chemie - International Edition, 2005, 44, 123-126.	13.8	229

#	Article	IF	CITATIONS
19	Ultrasmall Biocompatible WO _{3â^'} <i>_x</i> Nanodots for Multiâ€Modality Imaging and Combined Therapy of Cancers. Advanced Materials, 2016, 28, 5072-5079.	21.0	227
20	Biocompatible Semiconductor Quantum Dots as Cancer Imaging Agents. Advanced Materials, 2018, 30, e1706356.	21.0	227
21	Lateral Flow Immunochromatographic Assay for Sensitive Pesticide Detection by Using Fe ₃ O ₄ Nanoparticle Aggregates as Color Reagents. Analytical Chemistry, 2011, 83, 6778-6784.	6.5	216
22	Electroluminescence Studies on Self-Assembled Films of PPV and CdSe Nanoparticles. Journal of Physical Chemistry B, 1998, 102, 4096-4103.	2.6	214
23	Size-Dependent Electrochemical Behavior of Thiol-Capped CdTe Nanocrystals in Aqueous Solution. Journal of Physical Chemistry B, 2005, 109, 1094-1100.	2.6	211
24	NaGdF ₄ Nanoparticle-Based Molecular Probes for Magnetic Resonance Imaging of Intraperitoneal Tumor Xenografts <i>in Vivo</i> . ACS Nano, 2013, 7, 330-338.	14.6	207
25	Dual-Ratiometric Target-Triggered Fluorescent Probe for Simultaneous Quantitative Visualization of Tumor Microenvironment Protease Activity and pH <i>in Vivo</i>). Journal of the American Chemical Society, 2018, 140, 211-218.	13.7	207
26	Few‣ayer Graphdiyne Nanosheets Applied for Multiplexed Realâ€Time DNA Detection. Advanced Materials, 2017, 29, 1606755.	21.0	198
27	Ultrasmall Biocompatible Bi ₂ Se ₃ Nanodots for Multimodal Imaging-Guided Synergistic Radiophotothermal Therapy against Cancer. ACS Nano, 2016, 10, 11145-11155.	14.6	196
28	Anchoring Group Effects of Surface Ligands on Magnetic Properties of Fe ₃ O ₄ Nanoparticles: Towards High Performance MRI Contrast Agents. Advanced Materials, 2014, 26, 2694-2698.	21.0	194
29	Ultrasmall Magnetic CuFeSe ₂ Ternary Nanocrystals for Multimodal Imaging Guided Photothermal Therapy of Cancer. ACS Nano, 2017, 11, 5633-5645.	14.6	181
30	Boosting H ₂ O ₂ â€Guided Chemodynamic Therapy of Cancer by Enhancing Reaction Kinetics through Versatile Biomimetic Fenton Nanocatalysts and the Second Nearâ€Infrared Light Irradiation. Advanced Functional Materials, 2020, 30, 1906128.	14.9	177
31	Coating Aqueous Quantum Dots with Silica via Reverse Microemulsion Method:  Toward Size-Controllable and Robust Fluorescent Nanoparticles. Chemistry of Materials, 2007, 19, 4123-4128.	6.7	176
32	Incorporating Fluorescent CdTe Nanocrystals into a Hydrogel via Hydrogen Bonding:Â Toward Fluorescent Microspheres with Temperature-Responsive Properties. Chemistry of Materials, 2005, 17, 2648-2653.	6.7	169
33	Are Rareâ€Earth Nanoparticles Suitable for In Vivo Applications?. Advanced Materials, 2014, 26, 6922-6932.	21.0	166
34	Tumor Microenvironmentâ€Triggered Aggregation of Antiphagocytosis ^{99m} Tc‣abeled Fe ₃ O ₄ Nanoprobes for Enhanced Tumor Imaging In Vivo. Advanced Materials, 2017, 29, 1701095.	21.0	162
35	Metformin-Induced Stromal Depletion to Enhance the Penetration of Gemcitabine-Loaded Magnetic Nanoparticles for Pancreatic Cancer Targeted Therapy. Journal of the American Chemical Society, 2020, 142, 4944-4954.	13.7	153
36	Small is Smarter: Nano MRI Contrast Agents – Advantages and Recent Achievements. Small, 2016, 12, 556-576.	10.0	147

#	Article	IF	CITATIONS
37	Magnetically Engineered Semiconductor Quantum Dots as Multimodal Imaging Probes. Advanced Materials, 2014, 26, 6367-6386.	21.0	145
38	White-light electroluminescence from self-assembled Q-CdSe/PPV multilayer structures. Advanced Materials, 1997, 9, 802-805.	21.0	144
39	Coordinatively Unsaturated Fe ³⁺ Based Activatable Probes for Enhanced MRI and Therapy of Tumors. Angewandte Chemie - International Edition, 2019, 58, 11088-11096.	13.8	143
40	Monodisperse Dual Plasmonic Au@Cu _{2–<i>x</i>} E (E= S, Se) Core@Shell Supraparticles: Aqueous Fabrication, Multimodal Imaging, and Tumor Therapy at <i>in Vivo</i> Level. ACS Nano, 2017, 11, 8273-8281.	14.6	139
41	Lateral Patterning of CdTe Nanocrystal Films by the Electric Field Directed Layer-by-Layer Assembly Method. Langmuir, 2002, 18, 4098-4102.	3.5	127
42	Facile synthesis of ultrasmall PEGylated iron oxide nanoparticles for dual-contrast <i>T</i> ₁ - and <i>T</i> ₂ -weighted magnetic resonance imaging. Nanotechnology, 2011, 22, 245604.	2.6	126
43	Multispectral optoacoustic imaging of dynamic redox correlation and pathophysiological progression utilizing upconversion nanoprobes. Nature Communications, 2019, 10, 1087.	12.8	126
44	Quantitatively Visualizing Tumor-Related Protease Activity <i>in Vivo</i> Using a Ratiometric Photoacoustic Probe. Journal of the American Chemical Society, 2019, 141, 3265-3273.	13.7	123
45	Recent advancements in biocompatible inorganic nanoparticles towards biomedical applications. Biomaterials Science, 2018, 6, 726-745.	5.4	121
46	Investigations on Iron Sulfide Nanosheets Prepared via a Single-Source Precursor Approach. Crystal Growth and Design, 2008, 8, 1023-1030.	3.0	119
47	Superdispersible PVP-Coated Fe ₃ O ₄ Nanocrystals Prepared by a "One-Pot― Reaction. Journal of Physical Chemistry B, 2008, 112, 14390-14394.	2.6	115
48	Magnetically engineered Cd-free quantum dots as dual-modality probes for fluorescence/magnetic resonance imaging of tumors. Biomaterials, 2014, 35, 1608-1617.	11.4	110
49	Radiolabeling nanomaterials for multimodality imaging: New insights into nuclear medicine and cancer diagnosis. Biomaterials, 2020, 228, 119553.	11.4	109
50	Highly Fluorescent CdTe@SiO ₂ Particles Prepared via Reverse Microemulsion Method. Chemistry of Materials, 2010, 22, 420-427.	6.7	107
51	Incorporating CdTe Nanocrystals into Polystyrene Microspheres: Towards Robust Fluorescent Beads. Small, 2006, 2, 898-901.	10.0	105
52	Diameter-Tunable CdTe Nanotubes Templated by 1D Nanowires of Cadmium Thiolate Polymer. Angewandte Chemie - International Edition, 2006, 45, 6462-6466.	13.8	105
53	Monitoring the Opening and Recovery of the Blood–Brain Barrier with Noninvasive Molecular Imaging by Biodegradable Ultrasmall Cu _{2–<i>x</i>} Se Nanoparticles. Nano Letters, 2018, 18, 4985-4992.	9.1	105
54	Magnetic Janus Particles Prepared by a Flame Synthetic Approach: Synthesis, Characterizations and Properties. Advanced Materials, 2009, 21, 184-187.	21.0	103

#	Article	IF	CITATIONS
55	Protease-Activated Ratiometric Fluorescent Probe for pH Mapping of Malignant Tumors. ACS Nano, 2015, 9, 3199-3205.	14.6	102
56	No king without a crown – impact of the nanomaterial-protein corona on nanobiomedicine. Nanomedicine, 2015, 10, 503-519.	3.3	101
57	Second near-infrared photodynamic therapy and chemotherapy of orthotopic malignant glioblastoma with ultra-small Cu _{2â^'x} Se nanoparticles. Nanoscale, 2019, 11, 7600-7608.	5.6	100
58	Engineering NIR-IIb fluorescence of Er-based lanthanide nanoparticles for through-skull targeted imaging and imaging-guided surgery of orthotopic glioma. Nano Today, 2020, 34, 100905.	11.9	100
59	Aqueous synthesis of CdTe nanocrystals: progresses and perspectives. Chemical Communications, 2011, 47, 9293.	4.1	99
60	Biocompatible near-infrared quantum dots delivered to the skin by microneedle patches record vaccination. Science Translational Medicine, 2019, 11, .	12.4	95
61	pHâ€Responsive Fe(III)–Gallic Acid Nanoparticles for In Vivo Photoacousticâ€Imagingâ€Guided Photothermal Therapy. Advanced Healthcare Materials, 2016, 5, 772-780.	7.6	94
62	Molecular Imaging of Vulnerable Atherosclerotic Plaques <i>in Vivo</i> with Osteopontin-Specific Upconversion Nanoprobes. ACS Nano, 2017, 11, 1816-1825.	14.6	91
63	Boosting the Radiosensitizing and Photothermal Performance of Cu2–xSe Nanocrystals for Synergetic Radiophotothermal Therapy of Orthotopic Breast Cancer. ACS Nano, 2019, 13, 1342-1353.	14.6	91
64	Ultrasensitive <i>in Vivo</i> Detection of Primary Gastric Tumor and Lymphatic Metastasis Using Upconversion Nanoparticles. ACS Nano, 2015, 9, 2120-2129.	14.6	90
65	Light-Enhanced O ₂ -Evolving Nanoparticles Boost Photodynamic Therapy To Elicit Antitumor Immunity. ACS Applied Materials & Interfaces, 2019, 11, 16367-16379.	8.0	90
66	Preparation and photoluminescence of water-dispersible ZnSe nanocrystals. Materials Letters, 2004, 58, 3898-3902.	2.6	82
67	Biodegradable Inorganic Nanoparticles for Cancer Theranostics: Insights into the Degradation Behavior. Bioconjugate Chemistry, 2020, 31, 315-331.	3.6	82
68	Insight into Strain Effects on Band Alignment Shifts, Carrier Localization and Recombination Kinetics in CdTe/CdS Core/Shell Quantum Dots. Journal of the American Chemical Society, 2015, 137, 2073-2084.	13.7	81
69	Ultra-small nanocluster mediated synthesis of Nd 3+ -doped core-shell nanocrystals with emission in the second near-infrared window for multimodal imaging of tumor vasculature. Biomaterials, 2018, 175, 30-43.	11.4	81
70	A Novel Type of Dual-Modality Molecular Probe for MR and Nuclear Imaging of Tumor: Preparation, Characterization and in Vivo Application. Molecular Pharmaceutics, 2009, 6, 1074-1082.	4.6	79
71	Materials aspects of semiconductor nanocrystals for optoelectronic applications. Materials Horizons, 2017, 4, 155-205.	12.2	78
72	Surface engineering of gold nanoparticles for in vitro siRNA delivery. Nanoscale, 2012, 4, 5102.	5.6	75

#	Article	IF	CITATIONS
73	MRI/optical dual-modality imaging of vulnerable atherosclerotic plaque with an osteopontin-targeted probe based on Fe 3 O 4 nanoparticles. Biomaterials, 2017, 112, 336-345.	11.4	71
74	Soybean Lecithinâ€Mediated Nanoporous PLGA Microspheres with Highly Entrapped and Controlled Released BMPâ€2 as a Stem Cell Platform. Small, 2018, 14, e1800063.	10.0	71
75	Red blood cell membrane-coated upconversion nanoparticles for pretargeted multimodality imaging of triple-negative breast cancer. Biomaterials Science, 2020, 8, 1802-1814.	5.4	71
76	Electric Field Directed Layer-by-Layer Assembly of Highly Fluorescent CdTe Nanoparticles. Journal of Nanoscience and Nanotechnology, 2001, 1, 133-136.	0.9	70
77	Nanopolymersomes with an Ultrahigh Iodine Content for Highâ€Performance Xâ€Ray Computed Tomography Imaging In Vivo. Advanced Materials, 2017, 29, 1603997.	21.0	70
78	A facile route for preparing rhabdophane rare earth phosphate nanorods. Journal of Materials Chemistry, 2006, 16, 1360.	6.7	69
79	Aqueous synthesis of PEGylated copper sulfide nanoparticles for photoacoustic imaging of tumors. Nanoscale, 2015, 7, 11075-11081.	5.6	68
80	Gelification: An Effective Measure for Achieving Differently Sized Biocompatible Fe ₃ O ₄ Nanocrystals through a Single Preparation Recipe. Journal of the American Chemical Society, 2011, 133, 19512-19523.	13.7	66
81	Investigations on the Interactions between Plasma Proteins and Magnetic Iron Oxide Nanoparticles with Different Surface Modifications. Journal of Physical Chemistry C, 2010, 114, 21270-21276.	3.1	64
82	Flow Synthesis of Biocompatible Fe ₃ O ₄ Nanoparticles: Insight into the Effects of Residence Time, Fluid Velocity, and Tube Reactor Dimension on Particle Size Distribution. Chemistry of Materials, 2015, 27, 1299-1305.	6.7	64
83	Enhanced Synergism of Thermo-chemotherapy For Liver Cancer with Magnetothermally Responsive Nanocarriers. Theranostics, 2018, 8, 693-709.	10.0	63
84	Polyhedral Maghemite Nanocrystals Prepared by a Flame Synthetic Method: Preparations, Characterizations, and Catalytic Properties. ACS Nano, 2009, 3, 1775-1780.	14.6	60
85	Penetration of Quantum Dot Particles Through Human Skin. Journal of Biomedical Nanotechnology, 2010, 6, 586-595.	1.1	60
86	X-ray-Based Techniques to Study the Nano–Bio Interface. ACS Nano, 2021, 15, 3754-3807.	14.6	60
87	Ultrasmall superparamagnetic iron oxide nanoparticles: A next generation contrast agent for magnetic resonance imaging. Wiley Interdisciplinary Reviews: Nanomedicine and Nanobiotechnology, 2022, 14, e1740.	6.1	60
88	Constructing PbI2 nanoparticles into a multilayer structure using the molecular deposition (MD) method. Journal of the Chemical Society Chemical Communications, 1994, , 2777.	2.0	59
89	Aqueous Manganese-Doped Core/Shell CdTe/ZnS Quantum Dots with Strong Fluorescence and High Relaxivity. Journal of Physical Chemistry C, 2013, 117, 18752-18761.	3.1	58
90	A Bio-inspired Route to Fabricate Submicrometer-Sized Particles with Unusual Shapes â^ Mineralization of Calcium Carbonate within Hydrogel Spheres. Chemistry of Materials, 2005, 17, 656-660.	6.7	57

#	Article	IF	CITATIONS
91	Quantitative Mapping of Glutathione within Intracranial Tumors through Interlocked MRI Signals of a Responsive Nanoprobe. Angewandte Chemie - International Edition, 2021, 60, 8130-8138.	13.8	57
92	Synthesis, optical properties, and superlattice structure of Cu(I)-doped CdS nanocrystals. Applied Physics Letters, 2010, 97, .	3.3	56
93	Preparation of magnetite nanocrystals with surface reactive moieties by one-pot reaction. Journal of Colloid and Interface Science, 2007, 311, 469-474.	9.4	55
94	Synthesis and self-assembly of Cu1.94S–ZnS heterostructured nanorods. CrystEngComm, 2010, 12, 4124.	2.6	54
95	In vivo multimodality imaging of miRNA-16 iron nanoparticle reversing drug resistance to chemotherapy in a mouse gastric cancer model. Nanoscale, 2014, 6, 14343-14353.	5.6	54
96	Biodegradable Nanoagents with Short Biological Half‣ife for SPECT/PAI/MRI Multimodality Imaging and PTT Therapy of Tumors. Small, 2018, 14, 1702700.	10.0	51
97	Near-Infrared Afterglow Luminescence of Chlorin Nanoparticles for Ultrasensitive <i>In Vivo</i> Imaging. Journal of the American Chemical Society, 2022, 144, 6719-6726.	13.7	51
98	In situ111In-doping for achieving biocompatible and non-leachable 111In-labeled Fe3O4 nanoparticles. Chemical Communications, 2014, 50, 2170.	4.1	50
99	Longer and Stronger: Improving Persistent Luminescence in Size-Tuned Zinc Gallate Nanoparticles by Alcohol-Mediated Chromium Doping. ACS Nano, 2020, 14, 12113-12124.	14.6	50
100	Ultra-sensitive Nanoprobe Modified with Tumor Cell Membrane for UCL/MRI/PET Multimodality Precise Imaging of Triple-Negative Breast Cancer. Nano-Micro Letters, 2020, 12, 62.	27.0	50
101	Oral administration of highly bright Cr ³⁺ doped ZnGa ₂ O ₄ nanocrystals for <i>in vivo</i> targeted imaging of orthotopic breast cancer. Journal of Materials Chemistry B, 2018, 6, 1508-1518.	5.8	49
102	Preparations of bifunctional polymeric beads simultaneously incorporated with fluorescent quantum dots and magnetic nanocrystals. Nanotechnology, 2008, 19, 105601.	2.6	48
103	Upconversion luminescence nanoparticles-based lateral flow immunochromatographic assay for cephalexin detection. Journal of Materials Chemistry C, 2014, 2, 9637-9642.	5.5	48
104	"Smart―Nanoprobes for Visualization of Tumor Microenvironments. Advanced Healthcare Materials, 2018, 7, e1800391.	7.6	47
105	Preparation of bioconjugates of CdTe nanocrystals for cancer marker detection. Nanotechnology, 2006, 17, 2972-2977.	2.6	46
106	Amphiphilic ABC Triblock Copolymer-Assisted Synthesis of Core/Shell Structured CdTe Nanowires. Langmuir, 2005, 21, 4205-4210.	3.5	45
107	Cationic Gemini Surfactant-Assisted Synthesis of Hollow Au Nanostructures by Stepwise Reductions. ACS Applied Materials & Interfaces, 2013, 5, 5709-5716.	8.0	44
108	Emitting/Sensitizing Ions Spatially Separated Lanthanide Nanocrystals for Visualizing Tumors Simultaneously through Up―and Downâ€Conversion Nearâ€Infrared II Luminescence In Vivo. Small, 2019, 15, e1905344.	10.0	41

#	Article	IF	CITATIONS
109	Twoâ€Pronged Intracellular Coâ€Delivery of Antigen and Adjuvant for Synergistic Cancer Immunotherapy. Advanced Materials, 2022, 34, e2202168.	21.0	41
110	A monolayer of Pbl2nanoparticles adsorbed on MD–LB film. Journal of the Chemical Society Chemical Communications, 1994, , 2229-2230.	2.0	40
111	Quantum dot-antisense oligonucleotide conjugates for multifunctional gene transfection, mRNA regulation, and tracking of biological processes. Biomaterials, 2011, 32, 1923-1931.	11.4	40
112	Optical/MRI dual-modality imaging of M1 macrophage polarization in atherosclerotic plaque with MARCO-targeted upconversion luminescence probe. Biomaterials, 2019, 219, 119378.	11.4	40
113	Recent advances in molecular imaging of atherosclerotic plaques and thrombosis. Nanoscale, 2020, 12, 8040-8064.	5.6	38
114	Investigation on Photovoltaic Performance based on Matchstick-Like Cu2S–In2S3 Heterostructure Nanocrystals and Polymer. Nanoscale Research Letters, 2008, 3, 502-507.	5.7	36
115	Synthesis of Cu ₃ SnS ₄ nanocrystals and nanosheets by using Cu ₃₁ S ₁₆ as seeds. CrystEngComm, 2012, 14, 401-404.	2.6	36
116	Detection of early primary colorectal cancer with upconversion luminescent NP-based molecular probes. Nanoscale, 2016, 8, 12579-12587.	5.6	36
117	An adaptive Fuzzy C-means method utilizing neighboring information for breast tumor segmentation in ultrasound images. Medical Physics, 2017, 44, 3752-3760.	3.0	35
118	Nanoparticles weaponized with builtâ€in functions for imagingâ€guided cancer therapy. View, 2020, 1, e19.	5.3	35
119	Effect of the surface chemical modification on the optical properties of polymer-stabilized PbS nanoparticles. Journal of the Chemical Society, Faraday Transactions, 1995, 91, 4121.	1.7	34
120	Assembly of modified CdS particles/cationic polymer based on electrostatic interactions. Thin Solid Films, 1996, 284-285, 242-245.	1.8	34
121	A general approach for encapsulating aqueous colloidal particles into polymeric microbeads. Journal of Materials Chemistry, 2007, 17, 2930.	6.7	34
122	Revisiting the coordination chemistry for preparing manganese oxide nanocrystals in the presence of oleylamine and oleic acid. Nanoscale, 2014, 6, 5918.	5.6	34
123	Furin Enzyme and pH Synergistically Triggered Aggregation of Gold Nanoparticles for Activated Photoacoustic Imaging and Photothermal Therapy of Tumors. Analytical Chemistry, 2021, 93, 9277-9285.	6.5	34
124	Bright, Magnetic NIR-II Quantum Dot Probe for Sensitive Dual-Modality Imaging and Intensive Combination Therapy of Cancer. ACS Nano, 2022, 16, 8076-8094.	14.6	31
125	Polymer Langmuir-Blodgett film of organic-inorganic (Fe2O3) composite microgel. Thin Solid Films, 1994, 248, 106-109.	1.8	30
126	Healing Diabetic Ulcers with MoO _{3â^'} <i>_X</i> Nanodots Possessing Intrinsic ROS‣cavenging and Bacteriaâ€Killing Capacities. Small, 2022, 18, e2107137.	10.0	30

#	Article	IF	CITATIONS
127	Layer-by-layer depositions of polyelectrolyte/CdTe nanocrystal films controlled by electric fields. Journal of Materials Chemistry, 2002, 12, 1775-1778.	6.7	29
128	Generation, Characterization, and Application of Hierarchically Structured Self-Assembly Induced by the Combined Effect of Self-Emulsification and Phase Separation. Journal of the American Chemical Society, 2016, 138, 2090-2093.	13.7	29
129	Decorating multi-walled carbon nanotubes with quantum dots for construction of multi-color fluorescent nanoprobes. Nanotechnology, 2010, 21, 045606.	2.6	28
130	Differently sized magnetic/upconversion luminescent NaGdF ₄ :Yb,Er nanocrystals: flow synthesis and solvent effects. Chemical Communications, 2016, 52, 5872-5875.	4.1	28
131	Detection of lymph node metastasis with near-infrared upconversion luminescent nanoprobes. Nanoscale, 2018, 10, 21772-21781.	5.6	28
132	Characterizing viscoelastic properties of breast cancer tissue in a mouse model using indentation. Journal of Biomechanics, 2018, 69, 81-89.	2.1	27
133	Electrosprayed Soft Capsules of Millimeter Size for Specifically Delivering Fish Oil/Nutrients to the Stomach and Intestines. ACS Applied Materials & amp; Interfaces, 2020, 12, 6536-6545.	8.0	27
134	Restructuring and Remodeling of NaREF ₄ Nanocrystals by Electron Irradiation. Small, 2014, 10, 4711-4717.	10.0	26
135	NIR nanoprobe-facilitated cross-referencing manifestation of local disease biology for dynamic therapeutic response assessment. Chemical Science, 2020, 11, 803-811.	7.4	26
136	Rational Design and Synthesis of a Metalloproteinase-Activatable Probe for Dual-Modality Imaging of Metastatic Lymph Nodes in Vivo. Journal of Organic Chemistry, 2019, 84, 6126-6133.	3.2	25
137	Chemical Spacer Design for Engineering the Relaxometric Properties of Core–Shell Structured Rare Earth Nanoparticles. Chemistry of Materials, 2015, 27, 7918-7925.	6.7	24
138	Timely Visualization of the Collaterals Formed during Acute Ischemic Stroke with Fe ₃ O ₄ Nanoparticleâ€based MR Imaging Probe. Small, 2018, 14, e1800573.	10.0	24
139	Biocompatible off-stoichiometric copper indium sulfide quantum dots with tunable near-infrared emission <i>via</i> aqueous based synthesis. Chemical Communications, 2019, 55, 15053-15056.	4.1	24
140	An MRI contrast agent based on a zwitterionic metal-chelating polymer for hepatorenal angiography and tumor imaging. Journal of Materials Chemistry B, 2020, 8, 6956-6963.	5.8	24
141	Self-Illuminating Agents for Deep-Tissue Optical Imaging. Frontiers in Bioengineering and Biotechnology, 2019, 7, 326.	4.1	23
142	From Ultrathin Two-Dimensional Djurleite Nanosheets to One-Dimensional Nanorods Comprised of Djurleite Nanoplates: Synthesis, Characterization, and Formation Mechanism. Crystal Growth and Design, 2011, 11, 1109-1116.	3.0	22
143	A Cyclodextrinâ€Hosted Ir(III) Complex for Ratiometric Mapping of Tumor Hypoxia In Vivo. Advanced Science, 2021, 8, 2004044.	11.2	22
144	Facile synthesis of two-dimensional highly branched gold nanostructures in aqueous solutions of cationic gemini surfactant. CrystEngComm, 2013, 15, 2648.	2.6	21

#	Article	IF	CITATIONS
145	Bifunctional Superparticles Achieved by Assembling Fluorescent CuInS2@ZnS Quantum Dots and Amphibious Fe3O4Nanocrystals. Journal of Physical Chemistry C, 2013, 117, 21014-21020.	3.1	21
146	Doping Lanthanide Nanocrystals With Non-lanthanide Ions to Simultaneously Enhance Up- and Down-Conversion Luminescence. Frontiers in Chemistry, 2020, 8, 832.	3.6	21
147	Electroluminescence and photoluminescence in CdSe/poly (p-phenylene vinylene) composite films. Synthetic Metals, 1999, 102, 1213-1214.	3.9	20
148	Detection of toxoplasmic lesions in mouse brain by USPIO-enhanced magnetic resonance imaging. Magnetic Resonance Imaging, 2007, 25, 1442-1448.	1.8	19
149	Ultrasmall PEGylated MnxFe3â^'xO4 (x = 0–0.34) nanoparticles: effects of Mn(ii) doping on T1- and T2-weighted magnetic resonance imaging. RSC Advances, 2013, 3, 23454.	3.6	19
150	Anchoring Group-Mediated Radiolabeling of Inorganic Nanoparticles─A Universal Method for Constructing Nuclear Medicine Imaging Nanoprobes. ACS Applied Materials & Interfaces, 2022, 14, 8838-8846.	8.0	19
151	Surface-biofunctionalized multicore/shell CdTe@SiO ₂ composite particles for immunofluorescence assay. Nanotechnology, 2011, 22, 505104.	2.6	18
152	Coordinatively Unsaturated Fe 3+ Based Activatable Probes for Enhanced MRI and Therapy of Tumors. Angewandte Chemie, 2019, 131, 11205-11213.	2.0	18
153	Viscoelastic characterization of injured brain tissue after controlled cortical impact (CCI) using a mouse model. Journal of Neuroscience Methods, 2020, 330, 108463.	2.5	18
154	Manganese-Mediated Growth of ZnS Shell on KMnF ₃ :Yb,Er Cores toward Enhanced Up/Downconversion Luminescence. ACS Applied Materials & Interfaces, 2020, 12, 11934-11944.	8.0	18
155	Monodispersed Magnetic Polystyrene Beads with Excellent Colloidal Stability and Strong Magnetic Response. Macromolecular Rapid Communications, 2010, 31, 1805-1810.	3.9	16
156	Narrowing the Photoluminescence of Aqueous CdTe Quantum Dots via Ostwald Ripening Suppression Realized by Programmed Dropwise Precursor Addition. Journal of Physical Chemistry C, 2018, 122, 11109-11118.	3.1	16
157	Magnetic Ni/SiO2composite microcapsules prepared by one-pot synthesis. Journal of Materials Chemistry, 2009, 19, 1245-1251.	6.7	15
158	The Yin and Yang of coordinating co-solvents in the size-tuning of Fe ₃ O ₄ nanocrystals through flow synthesis. Nanoscale, 2017, 9, 18609-18612.	5.6	14
159	Sequential SPECT and NIR-II imaging of tumor and sentinel lymph node metastasis for diagnosis and image-guided surgery. Biomaterials Science, 2021, 9, 3069-3075.	5.4	14
160	An APNâ€Activated Chemiluminescent Probe for Imageâ€Guided Surgery of Malignant Tumors. Advanced Optical Materials, 2022, 10, .	7.3	14
161	Layer-by-layer deposition of J-aggregates and polyelectrolytes for electroluminescence applications: A spectroscopic study. Israel Journal of Chemistry, 2000, 40, 129-138.	2.3	13
162	Template synthesis of braided gold nanowires with gemini surfactant–HAuCl4 aggregates. Journal of Nanoparticle Research, 2013, 15, 1.	1.9	13

#	Article	IF	CITATIONS
163	Two-Dimensional and Subnanometer-Thin Quasi-Copper-Sulfide Semiconductor Formed upon Copper–Copper Bonding. ACS Nano, 2021, 15, 873-883.	14.6	12
164	Molecular mechanisms for delicately tuning the morphology and properties of Fe ₃ O ₄ nanoparticle clusters. CrystEngComm, 2018, 20, 2421-2429.	2.6	11
165	A Novel Histochemical Staining Approach for Rareâ€Earthâ€Based Nanoprobes. Advanced Therapeutics, 2018, 1, 1800005.	3.2	11
166	Anchoring Group Mediated Radiolabeling for Achieving Robust Nanoimaging Probes. Small, 2021, 17, e2104977.	10.0	11
167	Regional biomechanical imaging of liver cancer cells. Journal of Cancer, 2019, 10, 4481-4487.	2.5	10
168	Turning-on persistent luminescence out of chromium-doped zinc aluminate nanoparticles by instilling antisite defects under mild conditions. Nanoscale, 2021, 13, 8514-8523.	5.6	10
169	Site-Selective Deposition of Enzyme/Polyelectrolyte Multilayer Films on ITO Electrodes Controlled Electric Fields. Chemistry Letters, 2002, 31, 1168-1169.	1.3	9
170	Detection of Epstein–Barr virus infection in cancer by using highly specific nanoprobe based on dBSA capped CdTe quantum dots. RSC Advances, 2014, 4, 22545.	3.6	9
171	Upconversion luminescence mediated photodynamic therapy through hydrophilically engineered porphyrin. Chemical Engineering and Processing: Process Intensification, 2019, 142, 107551.	3.6	9
172	Recent Advances in Renal Clearable Inorganic Nanoparticles for Cancer Diagnosis. Particle and Particle Systems Characterization, 2021, 38, 2000270.	2.3	8
173	Rapidly liver-clearable rare-earth core–shell nanoprobe for dual-modal breast cancer imaging in the second near-infrared window. Journal of Nanobiotechnology, 2021, 19, 369.	9.1	8
174	Light-triggered crosslinking of gold nanoparticles for remarkably improved radiation therapy and computed tomography imaging of tumors. Nanomedicine, 2019, 14, 2941-2955.	3.3	7
175	Magnetic Iron Oxide Nanoparticles and Their Applications in Magnetic Resonance Imaging. Sheng Wu Wu Li Hsueh Bao, 2011, 27, 272-288.	0.1	7
176	Rational Constructed Ultra-Small Iron Oxide Nanoprobes Manifesting High Performance for T1-Weighted Magnetic Resonance Imaging of Glioblastoma. Nanomaterials, 2021, 11, 2601.	4.1	7
177	Photothermal Therapy: Ambient Aqueous Synthesis of Ultrasmall PEGylated Cu _{2â^'} <i>_x</i> Se Nanoparticles as a Multifunctional Theranostic Agent for Multimodal Imaging Guided Photothermal Therapy of Cancer (Adv. Mater. 40/2016). Advanced Materials, 2016, 28, 8788-8788.	21.0	6
178	MRI Probes: Timely Visualization of the Collaterals Formed during Acute Ischemic Stroke with Fe ₃ O ₄ Nanoparticleâ€based MR Imaging Probe (Small 23/2018). Small, 2018, 14, 1870108.	10.0	6
179	Quantitative Mapping of Glutathione within Intracranial Tumors through Interlocked MRI Signals of a Responsive Nanoprobe. Angewandte Chemie, 2021, 133, 8211-8219.	2.0	6
180	Imaging Tumor Metastases with Molecular Probes. Current Pharmaceutical Design, 2015, 21, 6260-6264.	1.9	6

#	Article	IF	CITATIONS
181	Synthesis and characterization of biodegradable poly(ester anhydride) based on É>-caprolactone and adipic anhydride initiated by potassium poly(ethylene glycol)ate. Journal of Polymer Science Part A, 2003, 41, 1511-1520.	2.3	5
182	One-pot synthesis of PVP-coated Ni0.6Fe2.4O4 nanocrystals. Science Bulletin, 2010, 55, 3472-3478.	1.7	5
183	Longitudinal Study of the Effects of Environmental pH on the Mechanical Properties of <i>Aspergillus niger</i> . ACS Biomaterials Science and Engineering, 2017, 3, 2974-2979.	5.2	5
184	Shape controllable preparations of PbS nanocrystals using cysteine as the precursor of S2â^' ions. Science Bulletin, 2006, 51, 2576-2580.	1.7	3
185	Halide perovskite nanocrystals can also stand luminescent in water. Science Bulletin, 2018, 63, 1241-1242.	9.0	2
186	Chemodynamic Therapy: Boosting H ₂ O ₂ â€Guided Chemodynamic Therapy of Cancer by Enhancing Reaction Kinetics through Versatile Biomimetic Fenton Nanocatalysts and the Second Nearâ€Infrared Light Irradiation (Adv. Funct. Mater. 3/2020). Advanced Functional Materials, 2020, 30, 2070019.	14.9	2
187	Quantitatively visualizing the activity of MMP-2 enzyme in vivo using a ratiometric photoacoustic probe. Methods in Enzymology, 2021, 657, 59-87.	1.0	2
188	A Pretargeting Strategy Enabled by Bioorthogonal Reactions Towards Advanced Nuclear Medicines: Application and Perspective. Chemical Research in Chinese Universities, 2021, 37, 870-879.	2.6	2
189	Ultra-Low-Field MRI and Spin-Lattice Relaxation Time of \$^{1}hbox{H}\$ in the Presence of \$hbox{Fe}_{3}hbox{O}_{4}\$ Magnetic Nano-Particles Detected With a High-\$T_{m C}\$ DC-SQUID. IEEE Transactions on Applied Superconductivity, 2013, 23, 1602504-1602504.	1.7	1
190	Nanoparticles: Are Rare-Earth Nanoparticles Suitable for In Vivo Applications? (Adv. Mater. 40/2014). Advanced Materials, 2014, 26, 6921-6921.	21.0	1
191	Enhancement Effect of Illumination on the Photoluminescence of Water-Soluble CdTe Nanocrystals: Toward Highly Fluorescent CdTe/CdS Core—Shell Structure ChemInform, 2004, 35, no.	0.0	0
192	Nanocrystals: Restructuring and Remodeling of NaREF ₄ Nanocrystals by Electron Irradiation (Small 22/2014). Small, 2014, 10, 4800-4800.	10.0	0
193	Super-stable centimetre-scale inverse opal belts integrated with CdTe QDs for narrow band fluorescence optical waveguiding. Journal of Materials Chemistry C, 2015, 3, 10964-10967.	5.5	0
194	Evaluation of the Laser-Induced Thermotherapy Treatment Effect of Breast Cancer Based on Tissue Viscoelastic Properties. Journal of Engineering and Science in Medical Diagnostics and Therapy, 2018, 1,	0.5	0